THE JOURNAL OF PHYSICAL CHEMISTRY Letters

Letter

pubs.acs.org/JPCL

Graphitic Phase of NaCl. Bulk Properties and Nanoscale Stability

Alexander G. Kvashnin,[†,‡,§] Pavel B. Sorokin,*[,†,‡,§,∥] and David Tománek[⊥]

[†]Technological Institute for Superhard and Novel Carbon Materials, 7a Centralnaya Street, Troitsk, Moscow 142190, Russian Federation

[‡]Moscow Institute of Physics and Technology, Dolgoprudny 141700, Russian Federation

[§]Emanuel Institute of Biochemical Physics, 4 Kosigina Street, Moscow 119334, Russian Federation

[∥]National University of Science and Technology MISiS, 4 Leninskiy Prospekt, Moscow 119049, Russian Federation

[⊥]Physics and Astronomy Department, Michigan State University, East Lansing, Michigan 48824, United States

Supporting Information

ABSTRACT: We applied the ab initio approach to evaluate the stability and physical properties of the nanometer-thickness NaCl layered films and found that the rock salt films with a (111) surface become unstable with thickness below 1 nm and spontaneously split to graphitic-like films for reducing the electrostatic energy penalty. The observed sodium chloride graphitic phase displays an uncommon atomic arrangement and exists only as nanometer-thin quasi-two-dimensional films. The graphitic bulk counterpart is unstable and transforms to another hexagonal wurtzite NaCl phase that locates in the negative-pressure region of the phase diagram. It was found that the layers in the graphitic NaCl film are weakly bounded with each other with a binding energy order of 0.1 eV per stoichiometry unit. The electronic band gap of the graphitic NaCl displays an unusual nonmonotonic quantum confinement response.

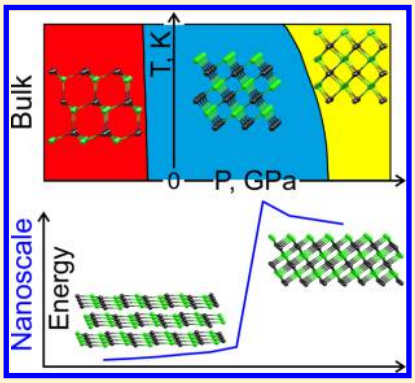

SECTION: Physical Processes in Nanomaterials and Nanostructures

Sodium chloride, also known as salt, table salt, or common salt, is one of the simplest and most thoroughly studied ionic crystals. In contrast with the covalently bounded systems, the sodium chloride displays a bare range of allotropes. It has been well established that NaCl with a rock salt structure (the B1 phase) transforms into a CsCl structure (the B2 phase) at about 30 GPa and room temperature.[1] A number of theoretical[2] and experimental[3] studies confirms that in the 0−300 GPa region, only these two phases occur, but the metallic low-symmetry NaCl[4] phase becomes favorable only at the extremely high pressures. Also, the stable Na_xCl_y phases of different stoichiometry were predicted and investigated in ref 5.

Another wurtzite-type phase of sodium chloride was predicted in ref 6. Despite the low energy, such a phase was not synthesized experimentally because of the negative value of the phase transition pressure. A completely different situation may occur in the nanoscale case; one phase, stable in the bulk, may become unstable or metastable if one or more dimensions are reduced to nanosize. For example, it was predicted that the graphitization effect greatly reduces the stability of the diamond nanofilms, which leads to its splitting into a multilayered graphene.[7,8] Also, the theoretical analysis in ref 9 reported that polar materials with favorable zinc blende or wurtzite-type structures tend to split into weakly bounded layers for the case of the few-atomic-layered films. The prediction was confirmed in the recent experimental works,[10,11] where the graphitic-like thin ZnO and SiC nanofilms were observed during growth by different techniques. The effect of graphitization of cubic thin films with diamond, zinc blende, and rock salt crystal structures was theoretically predicted in our recent study,[12] where the general tendency of graphitization in ultrathin slabs of cubic, zinc blende, and rock salt crystals was investigated.

Here, we show that the sodium chloride (111)-oriented nanofilms of rock salt structure spontaneously transform to films of a new graphitic phase (G-NaCl) to reduce the huge stress of the polar surface. Moreover, it was found that the energy of the considered G-NaCl films is practically equal to the energy of favorable B1-NaCl films with a (001) surface of the same number of layers. We investigated the atomic structure, properties, and stability of such a phase in both nanoscale and bulk states and found that G-NaCl is stable only in the case of the few-layered films with a thickness up to 1 nm. In the bulk case, G-NaCl transforms to a wurtzite-type structure.

The Letter is organized as follows. In the first part, the sodium chloride phase diagram calculation results are discussed, and a negative pressure region for the wurtzite NaCl phase (W-NaCl) is defined. The stability and electronic properties of W-NaCl are analyzed and compared with the rock salt B1 phase. The second part is devoted to the investigation of the transition

Received: September 26, 2014
Accepted: November 3, 2014
Published: November 3, 2014

   dx.doi.org/10.1021/jz502046f | J. Phys. Chem. Lett. 2014, 5, 4014−4019

from B1-NaCl films with a polar (111) surface to the films of a new graphitic phase. The relationship between the graphitic and wurtzite phases is discussed. The physical origin of the transition is investigated in detail, and the critical thickness below which a spontaneous conversion from rock salt to a layered graphitic structure occurs is determined. The in- and interlayer bond energy of the films is analyzed. The third part of the Letter is devoted to the investigation of the elastic properties of the films. Finally, the nonlinear electronic properties of the films of a new phase are discussed.

All calculations of the atomic structure and electronic properties of the considered phases were performed at a DFT level of theory within the local density approximation using the Perdew–Burke–Ernzerhof (PBE) parametrization[13−15] and a plane wave basis set implemented into the Quantum ESPRESSO package.[16] The plane wave energy cutoff was set to 30 Ry. To calculate the equilibrium atomic structures, the Brillouin zone was sampled according to the Monkhorst–Pack[17] scheme with an 8 × 8 × 3 k-point convergence grid for bulk phases and 8 × 8 × 1 k-points for nanoscale thin films. To avoid the spurious interactions between the neighboring layers of G-NaCl or B1-NaCl films, the vacuum space between them was greater than 15 Å.

The phase diagram was obtained from the calculations of the Gibbs free energies G of the compared phases in the quasiharmonic approximation[18]

$$G(P, T) = E_0(V) + PV + U_0(V) + F_{vib}(T, V)$$

where E_0, U_0, and F_{vib} are the total energy from the DFT calculations, while the zero-point (U_0) and vibrational (F_{vib}) energies are calculated from the following relations:

$$U_0(V) = \frac{1}{2}\int g(V, \omega)\hbar\omega \, d\omega$$

$$F_{vib}(T, V) = k_B T \int_\Omega g(V, \omega) \ln\left[1 - \exp\left(-\frac{\hbar\omega}{k_B T}\right)\right] d\omega$$

Here, $g(\omega)$ is the phonon density of states (PhDOS) at the given pressure, calculated using a density functional perturbation theory.[19] The PhDOS was calculated for each value of the equilibrium volume for each studied structure, using the density functional perturbation theory. Then, the PhDOS integrations above yielded the zero-point (U_0) and vibrational (F_{vib}) energies, for every chosen temperature. Substitution of all of the calculated energy contributions into the equation for Gibbs free energy allowed one to obtain the temperature-dependent phase transition pressure values.

The chosen approach is validated by refs 20 and 8, where the phase equilibrium lines for h-BN/c-BN and graphite/diamond were obtained, which appeared close to experimental data.

The GW calculations of band gaps of G-NaCl films with different numbers of layers were performed on top of PBE wave functions at the optimized geometry as implemented in the VASP[21−23] package. The plane wave energy cutoff was set to 400 eV. The k-point mesh in the lateral directions was 8 × 8, while for the perpendicular direction, the number of k-points was 1.

First, let us consider the bulk sodium chloride phases. The atomic structures of the bulk wurtzite (W) and cubic B1 and B2 phases of NaCl are shown at Figure 1a–c, respectively. Detailed crystal data, lattice constants, densities, and the main mechanical characteristics of these phases are summarized in Table S1 (see the Supporting Information).

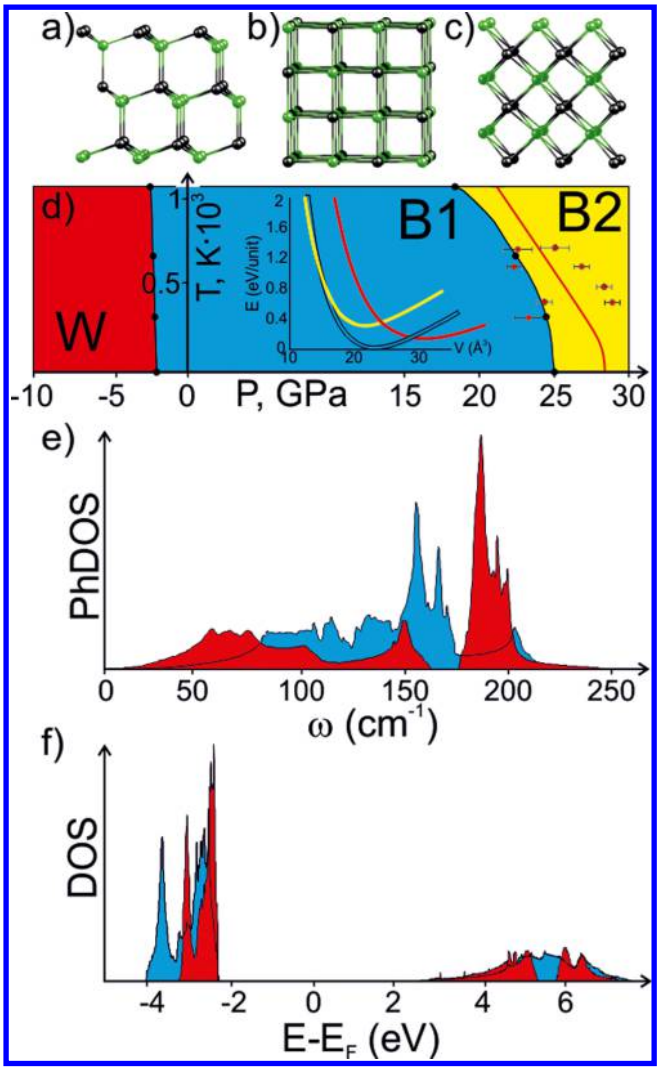

Figure 1. Atomic structures of the (a) wurtzite, (b) cubic B1, and (c) B2 NaCl phases. (d) The phase diagram of bulk NaCl. The stability regions of B1, B2, and W phases are marked by blue, yellow, and red, respectively. A red solid line and red points with error bars are experimental data of the B1/B2 phase boundary from ref 3. The inset shows the total energy per stoichiometry unit as a function of the unit volume for the considered bulk NaCl phases marked by corresponding colors. (e) PhDOS for cubic B1 (blue color) and W (red color) NaCl phases. (f) The electronic density of states for B1 and W phases. The Fermi level is marked as zero.

To obtain the temperature-dependent values of the phase transition pressure, we substitute the calculated energy contributions (total energy E_0, zero-point energy U_0, and vibration energy F_{vib}) into the equation for the Gibbs free energy. Figure 1d displays the phase diagram obtained for three NaCl phases, the subject of the present study. The general features of this phase diagram are very similar to those of the isostructural MgO.[24] A red solid line and red points with error bars represent the experimental data of the B1/B2 phase boundary from ref 3. As one can see from Figure 1d, the chosen approach has a good agreement with the corresponding experimental data where the calculated data (black line) are within the confidence interval of the experimental values of the phase transition pressure.

dx.doi.org/10.1021/jz502046f | J. Phys. Chem. Lett. 2014, 5, 4014−4019

The obtained phase diagram shows that W-NaCl (Figure 1a) is located in the negative range of the phase transition pressure due to the higher energy and lower density than the B1 phase (Figure 1b), which agrees with reference theoretical data.[6] The negative pressure is the reason why this simple and low-energy phase has not been yet experimentally produced. It was established that W-NaCl displays a lower density and a higher compressibility, which along with the pressure difference of ∼2 GPa at 0 K (Figure 1d) with cubic B1-NaCl allows us to draw an analogy with carbon where the phase transition pressure between graphite and diamond also equals ∼2 GPa at 0 K. Among other things, the W-NaCl is very similar to the graphite structure with the exception of bonding strength and interlayer interaction along the *c*-axis. On the other hand, the main difference between NaCl and carbon is that hexagonal W-NaCl phase is less stable than its cubic (B1-NaCl) counterpart, which could be seen from the inset of Figure 1d, where the total energies of the considered phases are shown as a function of the unit volume.

The stability of the considered phases could be described in terms of phonon frequencies. We calculated the PhDOS for both cubic (B1) and wurtzite (W) NaCl phases, as shown in Figure 1e at 1 atm. The obtained PhDOS for W-NaCl shows only positive frequencies, which validates the stability of such a phase. As one can see, the main PhDOS peak of B1-NaCl is located at 153 cm^{-1}, while the main peak of the W phase shifts toward the high-frequency region and equals 189 cm^{-1}.

The study of electronic properties of bulk B1 and W phases shows that both NaCl phases display wide insulating band gaps at about 5.0 and 4.8 eV, respectively (also the systematic underestimation of the band gap should be taken into account); see Figure 1f. Also, we calculate the fundamental gap of bulk B1 and W-NaCl phases by the GW approach. The obtained values show the significant scissor shift of the bands from 5.0 to 7.6 eV and from 4.8 to 7.7 eV, correspondingly. The GW band gap is in good agreement with the experimental data of 8.97 eV.[25]

The analogy between the carbon and sodium chloride phases can be drawn further. The known surface effect of graphitization leads to the transformation of the diamond nanometer thick slab into the multilayered graphene.[8] The fundamental difference in the bonding between sodium and chloride prevents the expectation of the same behavior in the considered case. However, we found that in the case of few-layered films, the W-NaCl thin films are more stable and more energy favorable compared to B1 films with the (111) orientation of the surface. The main reason for this instability is the charge transfer from the outermost anions to the cations to remove the huge dipole moment oriented along the (111) direction leading to a divergence of the surface energy that makes the surface intrinsically unstable.[26]

We performed a step-by-step investigation of the hexagonal phase of sodium chloride, where we gradually reduced the third dimension from the bulk to nanometer-thick films. It was found that cubic B1-NaCl films thinner than eight layers are unstable and spontaneously transform to graphitic hexagonal NaCl films (called G-NaCl) with an ABC stacking of the layers. The energies of thin cubic B1 films are higher than the energies of the corresponding G-NaCl films (Figure 2a). It can be seen from Figure 2a (black line) that the energy difference between the G-NaCl and the cubic B1-NaCl phases decreases as the number of layers increases (from 2 to 8) and approaches 0 at the number of layers equal to eight. At a further increase of the thickness, the cubic B1 films no longer spontaneously split to graphitic films and become energy-favorable.

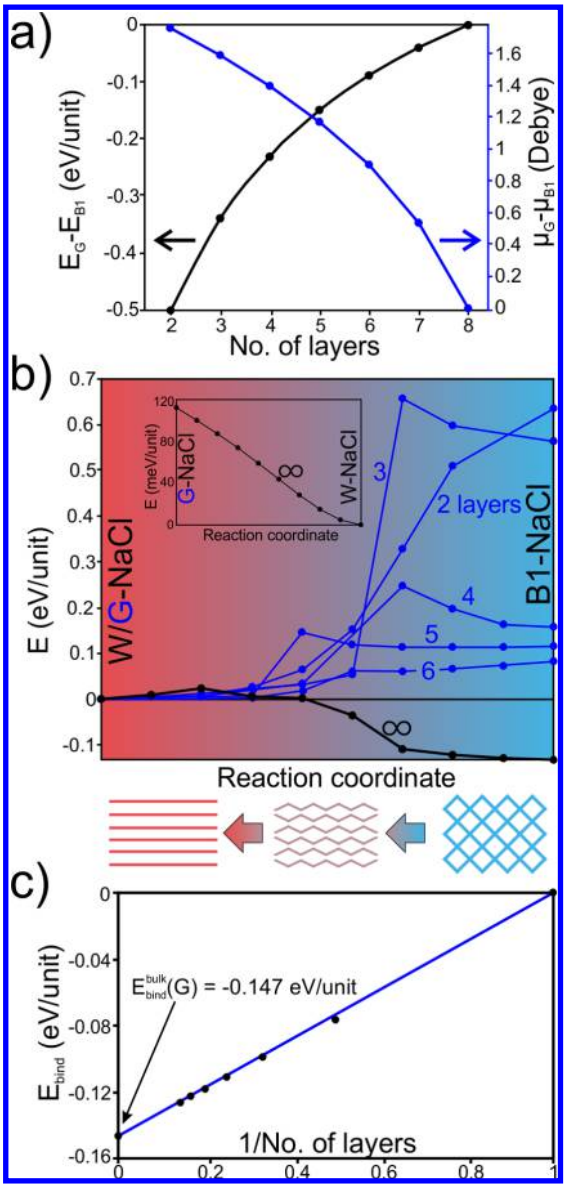

Figure 2. (a) The difference of the energy per stoichiometry unit (black line) and the dipole moments (blue line) of G-NaCl and B1-NaCl films as a function of the number of layers. b) Energy barriers show the transition from B1-NaCl films with different thicknesses (n = 2−6, ∞) into G-NaCl films. The transition of the bulk B1 phase to the W phase is shown by a bold black line. The inset shows the absence of the energy barrier for the transition from G- to W-NaCl phases in the bulk state. (c) The dependence of the interlayer binding energy on the inverse number of layers for thin G-NaCl films. Energies are given per stoichiometry unit.

The dominant impact of the electric dipole moment on the stability of B1 films was confirmed by the calculations of the dipole moment value along the direction normal to the (111) surface of the both G- and B1-NaCl films, as shown in Figure 2a (blue line). The dipole moment of the isolated NaCl films was calculated using the procedure developed in ref 27. The energetic benefit of the layered G-NaCl films comes from removing the surface dipole component normal to the (111) surface; thus, the electrostatic energy penalty reduces. The values of dipole moments for graphitic G and cubic B1 sodium

dx.doi.org/10.1021/jz502046f | *J. Phys. Chem. Lett.* 2014, 5, 4014−4019

chloride films become equal when the number of layers equals eight, which is closely correlated with the total energy difference for the films with different thicknesses (Figure 2a). Decreasing the dipole moment of the thick B1 films prevents the splitting and promotes the stability of such films.

Then, we compare the energies of G-NaCl films with the energies of B1 films with a lowest-energy (001) surface orientation.[28] It was found that B1-NaCl slabs with a (001) surface were a little more favorable than G-NaCl films with the corresponding thickness by 0.17 eV/unit, which means quite an equal probability of the formation of NaCl slabs with either G or B1 types of structures.

Further study is devoted to the investigations of the energy barriers of the spontaneous splitting of B1-NaCl films into graphitic G-NaCl films with different thicknesses (n = 2−6, ∞), as presented in Figure 2b. Transition paths show that cubic B1 films transform to graphitic films with a small barrier (0.089−0.031 eV/unit, which can be overcome by room temperature) in the thickness range of 3−5 layers and split without a barrier for the thicker films (>5 layers) and for bilayered films. In this case, a film consists only of the surface and is mostly exposed by the impact of the destabilizing dipole moment. Subsequent increasing of the thickness leads to further increasing of the stability of B1 films, which no longer split into G films.

The transition path between G-NaCl and W-NaCl phases in infinitely thick slabs, corresponding to bulk structures, is shown in the inset of Figure 2b. Because there are no energy barriers, the less stable graphitic phase transforms to the wurtzite phase spontaneously. This is the reason why we considered the bulk transition from the cubic B1 phase directly to the wurtzite phase instead of G-NaCl. As one can note from Figure 2b, the cubic B1-NaCl phase is more stable than the hexagonal W-NaCl phase by 0.13 eV/unit. The transition path from the bulk W phase to the B1 phase has a negligibly small energy barrier of 0.02 eV/unit, which allows the spontaneous transformation of the W-NaCl phase into the more stable B1 phase at a nonzero temperature. This fact explains why the W-NaCl phase has still not been obtained in experiment. Therefore, we can conclude that the sodium chloride phase with a hexagonal symmetry can only exist in the nanoscale state.

To determine the strength of the interaction between the layers of G-NaCl films, the interlayer binding energy of the films with a different number of layers was evaluated as $E_{bind} = (E_N^G - N{\cdot}E_1^G)/N$, where N is a number of layers in the graphitic film, E_1^G is total energy of a single layer, and E_N^G is total energy of the film consisting of N layers. One can see from Figure 2c that the interlayer binding energy increases as the thickness increases and approaches the bulk value of −0.147 eV/unit for a graphitic phase. Such behavior indicates a stronger interaction between the layers in the bulk G-NaCl than that in the nanoscale films, which means that thin G-NaCl films could be split easier compared to the bulk ones. The order of the value of the interlayer binding energy corresponds to the van-der-Waals interaction and is comparable with the values for graphite,[29] which manifests the relative independence of the monolayers in the films and their possible extraction using techniques such as mechanical[30] or liquid[31] exfoliation.

In addition to the stability of bulk and nanoscale sodium chloride phases, the elastic and electronic properties of these materials were studied in detail. The electronic properties of the nanoscale graphitic sodium chloride films were studied by both DFT-PBE and GW approaches, and the nonlinear behavior of the band gap dependence on the film thickness was found, as shown in Figure 3a. The DFT-PBE approach shows that all of the studied graphitic films are insulators with the band gap

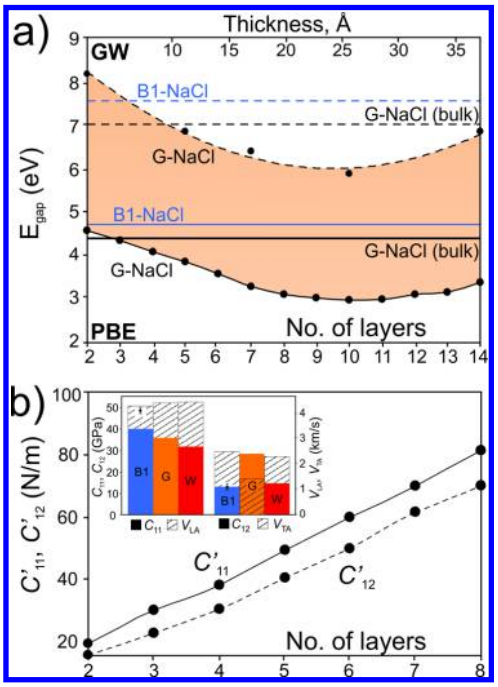

Figure 3. (a) The band gap dependence on the G-NaCl film thickness calculated using both DFT-PBE and GW approaches, denoted by solid and dashed lines, respectively. (b) Two-dimensional elastic constants C'_{11} (solid line) and C'_{12} (dashed line) of the nanoscale G-NaCl films depending on the number of layers. The inset shows the values of the elastic constants C_{11} and C_{12} (solid bars) and calculated velocities of longitudinal ν_{LA} and transverse ν_{TA} acoustic waves (dashed bars) for the bulk phases. Experimental values of the elastic constants for the B1 phase taken from ref 33 are shown by black points with error bars.

higher than 3 eV. As one can see, the band gap value decreases from 4.6 eV as the film thickness increases up to 24 Å, which corresponds to a G-NaCl film with eight layers with a band gap value of 3.1 eV. The nonlinear dependence of the band gap upon the thickness is similar to the already studied dependence of ultrathin diamond films.[32] The surface contribution to the electronic properties for the films thinner than 24 Å (eight layers) is higher than that for the thicker films, which relates with the stability of the films and with the electric dipole moment on the surface. Further increasing of the thickness leads to some changes in the band gap function behavior, where the band gap value increases with the thickness and approaches the value of the bulk G-NaCl phase (4.4 eV).

To get some more accurate results on the band gaps of the graphitic NaCl films, we used a GW approach. We calculated band gaps for the bulk G-NaCl and nanoscale graphitic films. The calculated fundamental gap for the bulk G-NaCl phase shows values of 7.1 eV compared to the DFT-PBE calculated value of 4.4 eV. In the case of nanoscale graphitic NaCl films, the GW approach was used to calculate the band gaps of G-NaCl films with a number of layers equal to 2, 5, 7, 10, and 14 (see Figure 3a) to confirm a general dependence of the band gap on the thickness. It was found that besides the scissor shift of bands, the GW approach does not change the band gap dependence on the film thickness, which allows the conclusion that the obtained nonlinear behavior of the band gap is correct.

dx.doi.org/10.1021/jz502046f | J. Phys. Chem. Lett. 2014, 5, 4014−4019

To evaluate the elastic properties of the graphitic NaCl films, the two-dimensional elastic constants C'_{11} and C'_{12} (N/m units) for nanoscale graphitic films and elastic constants C_{11} and C_{12} for bulk phases (B1, W, and G) were calculated as shown in Figure 3b. One can see that the calculated two-dimensional elastic moduli for the nanoscale graphitic films rise as the number of layers (thickness) increases.

We also calculated the C_{11} and C_{12} elastic constants for all considered bulk phases, as shown in the inset of Figure 3b. As one can see, the obtained values of the elastic constants for the bulk cubic B1 phase (C_{11} = 39.9 GPa, C_{12} = 13.1 GPa) are in good agreement with the corresponding experimental data (C_{11} = 48.2 ± 1.4 GPa, C_{12} = 12.8 ± 0.8 GPa),[33] which are depicted as black dots with error bars. The elastic constants C_{11}, C_{12} of bulk W- and G-NaCl phases were calculated as well, and their values equal 31.6, 14.6 GPa and 35.6, 28.2 GPa, respectively. It should be noted that the distinctive feature of the G-NaCl phase is a relatively high value of C_{12} compared to other bulk phases. The two-dimensional elastic constants can not be compared with the constants of the bulk phases due to the different dimensionalities. However, they can be used to calculate a more valuable characteristic of the material, such as velocities of acoustic waves, which could be compared with the corresponding data for bulk phases.

The velocities of longitudinal and transverse acoustic waves can be estimated from the obtained elastic constants using simple relations $\nu_{LA} = (C_{11}/\rho)^{1/2}$ and $\nu_{TA} = [(1/2)(C_{11} - C_{12})/\rho]^{1/2}$, where ρ is density.

The obtained velocities of the acoustic waves for the bulk sodium chloride phases are illustrated in the inset of Figure 3b. We calculated the velocities of longitudinal and transverse acoustic waves for the B1-NaCl phase (ν_{LA} = 4.31 km/s, ν_{TA} = 2.49 km/s), which agree well with the corresponding experimental data (ν_{LA} = 4.66 ± 0.06 km/s, ν_{TA} = 2.82 ± 0.08 km/s).[33] It should be noted that the calculated velocity of the longitudinal acoustic waves for the bulk W-NaCl phase (ν_{LA} = 4.45 km/s) is very close to the corresponding velocity of the graphitic phase (ν_{LA} = 4.43 km/s) and is slightly higher than that for its cubic counterpart (see the inset of Figure 3b). A relatively high value of the C_{12} elastic constant of the G-NaCl bulk phase leads to the lower velocity of the transverse acoustic waves (ν_{TA} = 1.43 km/s) compared to the other phases. In the case of nanoscale films, both velocities of longitudinal and transverse acoustic waves behave independently on the number of layers (thickness) and oscillate around the bulk values of the G-NaCl phase.

In summary, we performed density functional calculations to explore in detail the phase diagram of sodium chloride. We found that the stability region of a W-NaCl phase was located in the negative range of the phase diagram due to the higher energy and lower density than the B1 phase, which hides the wurtzite phase from the view of researchers. The electronic properties and stability of the W-NaCl phase were studied compared to the B1 phase. We found that in the nanoscale region, the B1-NaCl thin slabs become unstable due to the high dipole moment, which destabilized the (111) surface and transformed the B1 films to the new graphitic G-NaCl thin slabs instead of W-NaCl. We determined the critical thickness of the NaCl films below which a spontaneous splitting of the B1 films to G-NaCl films occurs, driven by the surface energy reduction due to the removal of the electrostatic dipole moment normal to the surface. Investigation of the elastic properties of both bulk and nanoscale phases shows that the graphitic phase displays a higher value of the C_{12} elastic constant. This work is in a trend of the "post-graphene" age, where scientists investigate different alternative layered materials that may overcome the outstanding graphene properties. We believe that our investigation of the new graphitic NaCl phase will open a novel family of ionic layered nanomaterials.

■ ASSOCIATED CONTENT

Supporting Information

Crystal data, density, and bulk modulus for NaCl phases considered in this study. This material is available free of charge via the Internet at http://pubs.acs.org.

■ AUTHOR INFORMATION

Corresponding Author

*E-mail: PBSorokin@tisnum.ru.

Notes

The authors declare no competing financial interest.

■ ACKNOWLEDGMENTS

We are grateful to the Moscow State University for the use of the "Chebishev" and "Lomonosov" cluster computers for our quantum chemical calculations. Part of the calculations were made on the Joint Supercomputer Center of the Russian Academy of Sciences. A.G.K. and P.B.S. acknowledge support from the Russian Science Foundation (Project #14-12-01217). A.G.K. acknowledges the Scholarship of President of Russia for Young Scientists and PhD Students (Competition SP-2013). D.T. acknowledges support from the National Science Foundation Cooperative Agreement #EEC-0832785, titled "NSEC: Center for High-rate Nanomanufacturing". The authors thank Zhen Zhu for fruitful discussions.

■ REFERENCES

(1) Bassett, W. A.; Takahashi, T.; Mao, H.; Weaver, J. S. Pressure-Induced Phase Transformation in NaCl. *J. Appl. Phys.* **1968**, *39*, 319–325.

(2) Froyen, S.; Cohen, M. L. Structural Properties of NaCl. *Phys. Rev. B* **1984**, *29*, 3770–3772.

(3) Li, X.; Jeanloz, R. Measurement of the B1–B2 Transition Pressure in NaCl at High Temperatures. *Phys. Rev. B* **1987**, *36*, 474–479.

(4) Chen, X.; Ma, Y. High-Pressure Structures and Metallization of Sodium Chloride. *Europhys. Lett.* **2012**, *100*, 26005(4).

(5) Zhang, W.; Oganov, A. R.; Goncharov, A. F.; Zhu, Q.; Boulfelfel, S. E.; Lyakhov, A. O.; Somayazulu, M.; Prakapenka, V. B. Unexpected Stable Stoichiometries of Sodium Chlorides. *Science* **2013**, *342*, 1502–1505.

(6) Čančarević, Ž. P.; Christian, S. J.; Jansen, M. Stability of Alkali Metal Halide Polymorphs as a Function of Pressure. *Chem.—Asian J.* **2008**, *3*, 561–572.

(7) Dong, X.; Zhou, X. F.; Qian, G. R.; Zhao, Z.; Tian, Y.; Wang, H. T. An Ab Initio Study on the Transition Paths from Graphite to Diamond under Pressure. *J. Phys.: Condens. Matter* **2013**, *25*, 145402.

(8) Kvashnin, A. G.; Chernozatonskii, L. A.; Yakobson, B. I.; Sorokin, P. B. Phase Diagram of Quasi-Two-Dimensional Carbon. *Nano Lett.* **2014**, *14*, 676–681.

(9) Freeman, C. L.; Claeyssens, F.; Allan, N. L.; Harding, J. H. Graphitic Nanofilms as Precursors to Wurtzite Films: Theory. *Phys. Rev. Lett.* **2006**, *96*, 066102.

(10) Claeyssens, F.; Freeman, C. L.; Allan, N. L.; Sun, Y.; Ashfolda, M. N. R.; Harding, J. H. Growth of ZnO Thin Films—Experiment and Theory. *J. Mater. Chem.* **2005**, *15*, 139–148.

(11) Lin, S. S. Light-Emitting Two-Dimensional Ultrathin Silicon Carbide. *J. Phys. Chem. C* **2012**, *116*, 3951−3955.
(12) Sorokin, P. B.; Kvashnin, A. G.; Zhu, Z.; Tománek, D. Spontaneous Graphitization of Ultrathin Cubic Structures: A Computational Study. *arXiv:1406.5922*; 2014.
(13) Hohenberg, P.; Kohn, W. Inhomogeneous Electron Gas. *Phys. Rev.* **1964**, *136*, B864−B871.
(14) Kohn, W.; Sham, L. J. Self-Consistent Equations Including Exchange and Correlation Effects. *Phys. Rev.* **1965**, *140*, A1133−A1138.
(15) Perdew, J. P.; Burke, K.; Ernzerhof, M. Generalized Gradient Approximation Made Simple. *Phys. Rev. Lett.* **1997**, *78*, 1396−1396.
(16) Giannozzi, P.; Baroni, S.; Bonini, N.; Calandra, M.; Car, R.; Cavazzoni, C.; Ceresoli, D.; Chiarotti, G. L.; Cococcioni, M.; Dabo, I.; Corso, A. D.; et al. Quantum Espresso: A Modular and Open-Source Software Project for Quantum Simulations of Materials. *J. Phys.: Condens. Matter* **2009**, *21*, 395502.
(17) Monkhorst, H. J.; Pack, J. D. Special Points for Brillouin-Zone Integrations. *Phys. Rev. B* **1976**, *13*, 5188−5192.
(18) Kern, G.; Kresse, G.; Hafner, J. Ab Initio Calculation of the Lattice Dynamics and Phase Diagram of Boron Nitride. *Phys. Rev. B* **1999**, *59*, 8551−8559.
(19) Baroni, S.; de Gironcoli, S.; Dal Corso, A.; Giannozzi, P. Phonons and Related Crystal Properties from Density-Functional Perturbation Theory. *Rev. Mod. Phys.* **2001**, *73*, 515−562.
(20) Kern, G.; Kresse, G.; Hafner, J. Ab Initio Calculation of the Lattice Dynamics and Phase Diagram of Boron Nitride. *Phys. Rev. B* **1999**, *59*, 8551−8559.
(21) Kresse, G.; Hafner, J. Ab Initio Molecular Dynamics for Liquid Metals. *Phys. Rev. B* **1993**, *47*, 558−561.
(22) Kresse, G.; Hafner, J. Ab Initio Molecular-dynamics Simulation of the Liquid−Metal−Amorphous-Semiconductor Transition in Germanium. *Phys. Rev. B* **1994**, *49*, 14251−14269.
(23) Kresse, G.; Furthmüller, J. Efficient Iterative Schemes for Ab Initio Total-Energy Calculations Using a Plane-Wave Basis Set. *Phys. Rev. B* **1996**, *54*, 11169−11186.
(24) Oganov, A. R.; Gillan, M. J.; Price, G. D. Ab Initio Lattice Dynamics and Structural Stability of MgO. *J. Chem. Phys.* **2003**, *118*, 10174−10182.
(25) Fong, C. Y.; Cohen, M. L. Band Structure and Ultraviolet Optical Properties of Sodium Chloride. *Phys. Rev. Lett.* **1968**, *21*, 22.
(26) Freeman, C. L.; Claeyssens, F.; Allan, N. L.; Harding, J. H. Graphitic Nanofilms as Precursors to Wurtzite Films: Theory. *Phys. Rev. Lett.* **2006**, *96*, 066102.
(27) Shi, N.; Ramprasad, R. Dielectric Properties of Ultrathin SiO_2 Slabs. *Appl. Phys. Lett.* **2005**, *87*, 262102.
(28) Tasker, P. W. The Surface Energies, Surface Tensions and Surface Structure of the Alkali Halide Crystals. *Philos. Mag. A* **1979**, *39*, 119−136.
(29) Chen, X.; Tian, F.; Persson, C.; Duan, W.; Chen, N. X. Interlayer Interactions in Graphites. *Sci. Rep.* **2013**, *3*, 3046.
(30) Novoselov, K. S.; Jiang, D.; Schedin, F.; Booth, T. J.; Khotkevich, V. V.; Morozov, S. V.; et al. Two-Dimensional Atomic Crystals. *Proc. Natl. Acad. Sci. U.S.A.* **2005**, 10451−10453.
(31) Hernandez, Y.; Nicolosi, V.; Lotya, M.; Blighe, F. M.; Sun, Z.; De, S.; McGovern, I. T.; Holland, B.; Byrne, M.; Gun'Ko, Y. K.; Boland, J. J.; et al. High-Yield Production of Graphene by Liquid-Phase Exfoliation of Graphite. *Nat. Nanotechnol.* **2008**, *3*, 563−568.
(32) Chernozatonskii, L. A.; Sorokin, P. B.; Kuzubov, A. A.; Sorokin, B. P.; Kvashnin, A. G.; Kvashnin, D. G.; Avramov, P. V.; Yakobson, B. I. Influence of Size Effect on the Electronic and Elastic Properties of Diamond Films with Nanometer Thickness. *J. Phys. Chem. C* **2011**, *115*, 132−136.
(33) Whitfield, C. H.; Brody, E. M.; Bassett, W. A. Elastic Moduli of NaCl by Brillouin Scattering at High Pressure in a Diamond Anvil Cell. *Rev. Sci. Instrum.* **1976**, *47*, 942−947.